PRS GLOBAL OPEN
ORIGINAL ARTICLE
Pediatric/Craniofacial

# Cortical Thickness in Crouzon–Pfeiffer Syndrome: Findings in Relation to Primary Cranial Vault Expansion

Alexander T. Wilson, BS*
Catherine A. de Planque, MD*
Sumin S. Yang, BS*
Robert C. Tasker, MA, MD, FRCP†
Marie-Lise C. van Veelen, MD, PhD‡
Marjolein H.G. Dremmen, MD§
Henri A. Vrooman, PhD§¶
Irene M.J. Mathijssen, MD, PhD*

**Background:** Episodes of intracranial hypertension are associated with reductions in cerebral cortical thickness (CT) in syndromic craniosynostosis. Here we focus on Crouzon–Pfeiffer syndrome patients to measure CT and evaluate associations with type of primary cranial vault expansion and synostosis pattern.
**Methods:** Records from 34 Crouzon–Pfeiffer patients were reviewed along with MRI data on CT and intracranial volume to examine associations. Patients were grouped according to initial cranial vault expansion (frontal/occipital). Data were analyzed by multiple linear regression controlled for age and brain volume to determine an association between global/lobar CT and vault expansion type. Synostosis pattern effect sizes on global/lobar CT were calculated as secondary outcomes.
**Results:** Occipital expansion patients demonstrated 0.02 mm thicker cortex globally ($P = 0.81$) with regional findings, including: thicker cortex in frontal (0.02 mm, $P = 0.77$), parietal (0.06 mm, $P = 0.44$) and occipital (0.04 mm, $P = 0.54$) regions; and thinner cortex in temporal (−0.03 mm, $P = 0.69$), cingulate (−0.04 mm, $P = 0.785$), and, insula (−0.09 mm, $P = 0.51$) regions. Greatest effect sizes were observed between left lambdoid synostosis and the right cingulate (d = −1.00) and right lambdoid synostosis and the left cingulate ($d = -1.23$). Left and right coronal synostosis yielded effect sizes of $d = -0.56$ and $d = -0.42$ on respective frontal lobes.
**Conclusions:** Both frontal and occipital primary cranial vault expansions correlate to similar regional CT in Crouzon–Pfeiffer patients. Lambdoid synostosis appears to be associated with cortical thinning, particularly in the cingulate gyri.
*(Plast Reconstr Surg Glob Open 2020;8:e3204; doi: 10.1097/GOX.0000000000003204; Published online 4 November 2020.)*

## INTRODUCTION

The Crouzon–Pfeiffer syndrome is a common form of syndromic craniosynostosis,[1] and mutations in the fibroblast growth factor receptor (*FGFR2*) gene are responsible for phenotypic severity in accelerated cranial suture fusion, facial anomalies, and exorbitism.[2] Clinically, a severe sequela of (CP) syndrome is intracranial hypertension (ICH), which may be due to factors such as cranial growth restriction, venous outflow obstruction, hydrocephalus, and obstructive sleep apnea.[3–5] Hence, cranial vault expansion is commonly performed, and at our center, it involves procedures such as fronto-orbital advancement, biparietal out-fracturing, and occipital expansion.[6] Compared with fronto-orbital advancement, occipital expansion has produced a greater gain in intracranial volume at our center while reducing the incidence of papilledema and tonsillar herniation.[7]

Cerebral cortical thickness is an important in vivo biomarker for brain development and cognitive ability.[8,9] As a subcomponent of cortical volume, cortical thickness is a general measure of neuronal density, dendritic arborization, and glial support.[10] Due to advancement in image-processing techniques, its use in recent years across a variety of disciplines has risen and demonstrated it to be of increasing importance in establishing a morphologic link to various pathologic and non-pathologic

*From the *Department of Plastic and Reconstructive and Hand Surgery, Erasmus Medical Center, Rotterdam, the Netherlands; †Department of Neurology, Department of Anesthesiology, Critical Care and Pain Medicine, Boston Children's Hospital; Harvard Medical School, Boston, Mass.; ‡Department of Neurological Surgery, Erasmus Medical Center, Rotterdam, the Netherlands; §Department of Radiology, Erasmus Medical Center, Rotterdam, the Netherlands; and ¶Department of Medical Informatics, Erasmus Medical Center, Rotterdam, the Netherlands.*

*Received for publication July 10, 2020; accepted September 1, 2020.*



DOI: 10.1097/GOX.0000000000003204

**Disclosure:** *The authors have no financial interest to declare in relation to the content of this article.*

neuropsychological outcomes.[9,11–15] More recently it has demonstrated sensitivity to evidence of ICH in the syndromic craniosynostosis population.[16] Almost two-thirds of patients with CP syndrome develop ICH and undergo cranial vault expansion,[17] yet they exhibit—on average—global cortical thinning.[16] Since most cases of CP syndrome develop with normal intelligence,[18,19] we wondered whether the apparent discrepancy between evidence of global cortical thinning and development of normal intelligence could be resolved by a better understanding of lobar cortical findings proximate to skull regions involved in cranial vault expansion procedures. Hence, the primary aim of this study was to compare differences in cortical thickness following frontal versus occipital primary vault expansion in CP syndrome patients. Our secondary aim was to determine whether any relationship between synostosis pattern and cortical thickness exists.

## METHODS

The Institution Research Ethics Board at Erasmus University Medical Center, Rotterdam, the Netherlands approved this study (approval no.: MEC-2014-461), which is a part of ongoing work at the Dutch Craniofacial Center and involves protocolized care, brain imaging, clinical assessment, and data summary and evaluation.[6,20,21] We reviewed the medical records of CP syndrome patients who were managed at our center between 2008 and 2018. Our usual practice in such patients involves scheduled primary vault expansion in the first year of life. Patients were included in this study if they had cranial magnetic resonance imaging (MRI) data that could be extracted and analyzed from three-dimensional T1-weighted fast spoiled gradient echo sequences. We excluded patients in whom the quality of imaging was not suitable for analysis.

Additional clinical and demographic data collected include sex, age at the time of MRI, birth weight, age at the time of vault expansion, initial type of vault expansion, and synostosis pattern. Initial type of vault expansion was classified as frontal or occipital. Suture-specific synostosis was noted in each patient as a binary variable for each of the 6 major sutures. Partial involvement of a suture was considered as positive. Fundoscopy to assess for papilledema was also performed in all cases by a pediatric ophthalmologist before surgery, 3 months postoperatively, biannually until the age of 4, annually until the age of 6 and then upon indication in older patients. When papilledema was detected, it was followed up with confirmatory fundoscopy and imaging 4–6 weeks later. Data from these examinations were collected to analyze the presence of ICH both pre and postoperatively.

### MRI Acquisition

All MRI scans were performed on a 1.5 T scanner (GE Healthcare, MR Signa Excite HD, Little Chalfont, UK) with the imaging protocol, including a three-dimensional fast spoiled gradient echo T1-weighted MR sequence. Imaging parameters for craniosynostosis patients were the following: 2 mm slice thickness, no slice gap; field of view (FOV): 22.4 cm; matrix size: 224 × 224; in plane resolution of 1 mm; echo time : 3.1 ms; and repetition time: 9.9 ms.[22] MRI was the imaging modality of choice in this study because of its ability to adequately distinguish between tissue densities (white matter, grey matter, and dura) critical to the calculation of cerebral cortical thickness.

### Cortical Thickness and Brain Volume

MRI dicom files were exported and converted to neuroimaging informatics technology initiative (NIfTI)-1 file format on a computer cluster with Scientific Linux as the operating system before analysis with FreeSurfer software modules (v6.0, see https://surfer.nmr.mgh.harvard.edu; developed by the Athinoula A. Martinos Center for Biomedical Imaging, Massachusetts General Hospital).[23] The processing methodologies used by FreeSurfer have previously been validated and described in detail.[24–26] Maps produced by FreeSurfer are not restricted by voxel resolution of the original data and are therefore able to detect submillimeter changes in cortical thickness as demonstrated by validation against histological analysis (within 0.07 mm and statistically indistinguishable from standard neuropathologic techniques) and manual measurements.[27–30] All T1-weighted images from the cohort were processed using the "auto-recon-all" pipeline in FreeSurfer. Estimates of vertex-wise cortical thickness were then generated by hemisphere and by cerebral lobes (ie, frontal, temporal, parietal, occipital, cingulate, and insula) as specified by the "–lobes" argument within the 'mris_annotation2label' command. Left and right hemisphere thickness outputs were averaged to generate a value for global cortical thickness. Similarly, lobar outputs from left and right hemispheres were averaged to generate a whole lobe thickness. Whole brain volume excluding ventricular volume was exported from FreeSurfer as 'BrainSegVolNotVent' via the 'mri_segstats' command.

### Statistical Analysis

All data were imported into R statistical software (R Core Team, R version 3.6.1, 2019, Vienna, Austria) for analysis. Multivariate linear regression was first used to determine the level of variance in global thickness attributable to age at the time of MRI, sex, and whole brain volume. Multivariate analysis of covariance (MANCOVA) was then performed to assess these effects by lobe. Finally, multiple linear regression was used to determine associations between type of initial cranial vault expansion and lobar thickness while controlling for age and brain volume. A post-hoc power analysis was also performed to assess the quantitative limits of our current dataset. Cohen's $d$ with 95% confidence intervals were calculated as a secondary analysis to determine effect of suture-specific synostosis on underlying cortical lobes. Homogeneity of variance among suture-specific groups was evaluated by Levene's test for age and $\chi^2$ for sex.

## RESULTS

### Patient Cohort

Following review of medical and imaging records, 43 CP patients were identified. Six patients were excluded

from further analysis since they did not undergo any primary vault expansion; either because they did not have synostosis ($n = 2$) or because of late referral and/or incomplete records ($n = 4$). An additional 3 patients underwent primary biparietal expansion and were also excluded. In total, 34 CP patients (19 men, 15 women) were therefore included in our cohort (mean ± SD age at the time of MRI of 8.9 ± 4.5 years). The interval between initial vault expansion and MRI was 7.1 ± 4.7 years. ICH was present in 8 (23.5%) patients preoperatively alone, 8 (23.5%) patients postoperatively alone, and 6 (17.6%) patients both pre and postoperatively. In 12 (35.3%) patients, no ICH was present. Birth weight data (range: 2920–4460 g; SD: 408 g) were also collected, and no patients were found to be of low enough weight (<1500 g) to impact thickness development as reported in previous studies.[31,32] Additionally, birth weight was found to be evenly distributed between both treatment groups and among all sutural involvement subgroups.

**Primary Cranial Vault Expansion**

Before assessing any effect of primary cranial vault expansion type on cortical thickness, we determined the level of variance explained by age, sex, and brain volume. Multivariate linear regression showed that these three variables accounted for 40% of the variance in cortical thickness ($R^2 = 0.40$), with univariate analyses yielding $R^2$ for age, sex, and brain volume as 0.39, 0.01, and 0.06, respectively. Further evaluation by lobe using MANCOVA yielded a Pillai trace test statistic of 0.64, 0.17, and 0.24 for age, sex, and brain volume, respectively. Univariate results of the MANCOVA test by lobe are available in Table 1.

Of the 34 patients, 13 (7 male, 6 female, median age at MRI 5.1 yrs) underwent occipital expansion as a primary procedure. 21 patients (12 men, 9 women, median age at MRI 11.5) underwent primary frontal expansion. Multiple linear regression did not find a correlation between global cortical thickness and primary cranial vault expansion type (Table 2). Primary occipital expansion was associated with a 0.02 mm thicker cortex globally (β = 0.02, 95% CI –0.12 to –0.15, $P = 0.82$), as well as thicker frontal (β = 0.02, 95% CI –0.15 to –0.20, $P = 0.78$), parietal (β = 0.06, 95% CI –0.09 to –0.20, $P = 0.44$), and occipital (β = 0.05, 95% CI –0.10 to –0.19, $P = 0.51$) lobar cortices. Also, in the occipital expansion group, there was an association with thinner temporal (β = –0.03, 95% CI –0.16 to –0.10, $P = 0.68$), cingulate (β = –0.04, 95% CI –0.29 to –0.22, $P = 0.78$), and insular (β = –0.09, 95% CI –0.36 to –0.17, $P = 0.48$) cortices. β-coefficients and 95% confidence intervals for each region are shown in Figure 1. Lastly, power analysis revealed the need for a cohort size of 59 patients to detect a 0.2 mm change in thickness at a level of 80%. Our cohort in this study was 80% powered to detect a 0.37 mm difference between surgical treatment groups.

**Synostosis Pattern**

Of the 34 patients, 14 suffered from pansynostosis, 7 had bicoronal involvement, 6 had bilambdoid involvement, 4 had isolated sagittal synostosis, and 3 had additional combinations involving multiple sutures. Cohen's *d* effect sizes and 95% confidence intervals for independent involvement of 5 major sutures are shown in Table 3 along with demographic data for each subgroup. Homogeneity of variance was found to be adequate in each subgroup, as

**Table 1. Univariate Results from MANCOVA Test to Assess Variability Attributable to Age, Sex, and Brain Volume**

| | df | Sum sq | Mean sq | F statistic | $\eta^2$ |
|---|---|---|---|---|---|
| Frontal | | | | | |
| Age | 1 | 0.37174 | 0.37174 | 13.7338 | 0.30632442 |
| Sex | 1 | 0.02775 | 0.02775 | 1.0252 | 0.0228668 |
| Brain vol | 1 | 0.00204 | 0.00204 | 0.0756 | 0.00168102 |
| Residuals | 30 | 0.81202 | 0.02707 | | |
| Temporal | | | | | |
| Age | 1 | 0.27837 | 0.278374 | 17.8413 | 0.37158609 |
| Sex | 1 | 0.00245 | 0.00245 | 0.157 | 0.00327042 |
| Brain vol | 1 | 0.00024 | 0.000242 | 0.0155 | 0.00032037 |
| Residuals | 30 | 0.46808 | 0.015603 | | |
| Parietal | | | | | |
| Age | 1 | 0.15166 | 0.151659 | 7.5828 | 0.2017265 |
| Sex | 1 | 0.00006 | 0.000056 | 0.0028 | 7.98E-05 |
| Brain vol | 1 | 0.00008 | 0.000083 | 0.0042 | 0.00010641 |
| Residuals | 30 | 0.60001 | 0.02 | | |
| Occipital | | | | | |
| Age | 1 | 0.57963 | 0.57963 | 33.9775 | 0.50018553 |
| Sex | 1 | 0.01966 | 0.01966 | 1.1522 | 0.01696539 |
| Brain vol | 1 | 0.04776 | 0.04776 | 2.7999 | 0.04121398 |
| Residuals | 30 | 0.51178 | 0.01706 | | |
| Cingulate | | | | | |
| Age | 1 | 0.64805 | 0.64805 | 10.7218 | 0.25127664 |
| Sex | 1 | 0.00488 | 0.00488 | 0.0807 | 0.00189218 |
| Brain vol | 1 | 0.11283 | 0.11283 | 1.8667 | 0.04374901 |
| Residuals | 30 | 1.81327 | 0.06044 | | |
| Insula | | | | | |
| Age | 1 | 1.30516 | 1.30516 | 21.2218 | 0.38340486 |
| Sex | 1 | 0.22115 | 0.22115 | 3.5959 | 0.0649652 |
| Brain vol | 1 | 0.03279 | 0.03279 | 0.5331 | 0.00963242 |
| Residuals | 30 | 1.84503 | 0.0615 | | |

Brain vol, whole brain volume; df, degrees of freedom; sum sq, sum of squares; mean sq, mean square; η2, eta squared.

**Table 2. Linear Regression Results for Global and Lobar Cortical Thickness**

| | Lobar Thickness by Type of Cranial Vault Expansion | | | | | | | | | | | | | | | | | | | |
|---|---|---|---|---|---|---|---|---|---|---|---|---|---|---|---|---|---|---|---|---|
| | Global | | | Frontal | | | Temporal | | | Parietal | | | Occipital | | | Cingulate | | | Insula | |
| Predictors | Estimates | CI | *P* | Estimates | CI | *P* | Estimates | CI | *P* | Estimates | CI | *P* | Estimates | CI | *P* | Estimates | CI | *P* | Estimates | CI | *P* |
| (Intercept) | 2.92 | 2.55– 3.29 | **<0.001** | 3.06 | 2.56–3.55 | **<0.001** | 3.21 | 2.84–3.57 | **<0.001** | 2.66 | 2.25–3.07 | **<0.001** | 2.70 | 2.31–3.10 | **<0.001** | 3.51 | 2.79–4.24 | **<0.001** | 3.34 | 2.60–4.09 | **<0.001** |
| Age at MRI | −0.02 | −0.04 to −0.00 | **0.012** | −0.02 | −0.04–0.00 | **0.036** | −0.02 | −0.04–0.01 | **0.004** | −0.01 | −0.03–0.01 | 0.211 | −0.02 | −0.04–0.01 | **0.008** | −0.03 | −0.06–0.00 | 0.062 | −0.06 | −0.09–0.03 | **0.001** |
| Brain volume | 0.00 | −0.00–0.00 | 0.917 | 0.00 | −0.00–0.00 | 0.937 | 0.00 | −0.00–0.00 | 0.788 | 0.00 | −0.00–0.00 | 0.991 | −0.00 | −0.00–0.00 | 0.245 | −0.00 | −0.00–0.00 | 0.254 | 0.00 | −0.00–0.00 | 0.193 |
| Occipital expansion | 0.02 | −0.12 to −0.15 | 0.815 | 0.02 | −0.15–0.20 | 0.778 | −0.03 | −0.16–0.10 | 0.680 | 0.06 | −0.09–0.20 | 0.444 | 0.05 | −0.10–0.19 | 0.511 | −0.04 | −0.29–0.22 | 0.783 | −0.09 | −0.36–0.17 | 0.482 |
| Observations | 34 | | | 34 | | | 34 | | | 34 | | | 34 | | | 34 | | | 34 | | |
| $R^2$/$R^2$ adjusted | 0.387/0.326 | | | 0.308/0.239 | | | 0.377/0.314 | | | 0.217/0.139 | | | 0.528/0.481 | | | 0.286/0.215 | | | 0.426/0.368 | | |

CI, 95% confidence interval.

assessed by Levene's test for age (left coronal $P = 0.49$; right coronal $P = 0.57$; sagittal $P = 0.19$; left lambdoid $P = 0.89$; right lambdoid $P = 0.77$) and $\chi^2$ test for sex (left coronal $P = 0.68$; right coronal $P = 0.64$; sagittal $P = 0.63$; left lambdoid $P = 0.98$; right lambdoid $P = 0.98$). For matched synostosis pattern to underlying cortical thickness, the largest effect was observed between coronal sutures and the frontal cortex, with left coronal synostosis yielding an effect size of $d = -0.56$ (95% CI −1.4 to −0.27) and $d = -0.65$ (95% CI −1.49 to −0.19) and right coronal synostosis yielding $d = -0.31$ (95% CI −1.22 to −0.61) and $d = -0.42$ (95% CI −1.34 to −0.50) for left and right frontal lobes, respectively. The overall largest effect sizes were observed between lambdoid suture involvement and the cingulate cortex, with left lambdoid synostosis corresponding to $d = -0.87$ (95% CI −1.65 to −0.10) and $d = -1.00$ (95% CI −1.78 to —0.21) and right lambdoid synostosis corresponding to $d = -1.23$ (95% CI −2.08 to −0.38) and $d = -1.05$ (95% CI −1.88 to —0.22) for left and right cingulate cortices respectively. These effects are demonstrated in Figure 2.

## DISCUSSION

The primary aim of this study was to determine any association between cortical thickness and frontal versus occipital primary vault expansion in CP syndrome patients. Our secondary aim was to determine any relationship between synostosis pattern and cortical thickness. We hypothesized that cortical lobes beneath growth-restricted regions of the calvaria may be at an increased risk for thinning in CP patients and that targeted vault expansion may confer a protective advantage to these regions. This study failed to find any difference in effect between frontal and occipital primary vault expansions on global or lobar cerebral cortical thickness. In regard to synostosis pattern and cortical thickness, we found that lambdoid synostosis was associated with thinning across all brain regions, but particularly within the cingulate and frontal cortices. This leads us to question our hypothesis of localized growth restriction affecting proximate cortical lobes and consider how cranial shape contributes to pressure elevations and subsequent thinning in distant regions of the brain.

Both frontal and occipital cranial vault procedures resulted in similar cortical thicknesses in this study. Previous work by Spruijt et al evaluated the effect of frontal versus occipital primary vault expansions on occipitofrontal head circumference in an Apert and Crouzon cohort and found that occipital-first expansion resulted in greater circumferences and reduced postoperative incidence of papilledema.[7] A recent study has highlighted the importance of papilledema in syndromic craniosynostosis patients, demonstrating an association with global thinning of the cortex.[16] The failure to find a direct association between primary cranial vault expansion type and cortical thickness in this study is most likely due to insufficient power. It is possible that occipital expansion resulted in fewer cases of papilledema than would otherwise be observed; however, the effect of surgery type alone was insufficient to result in detectable cortical thinning. This study was adequately powered to detect only a large

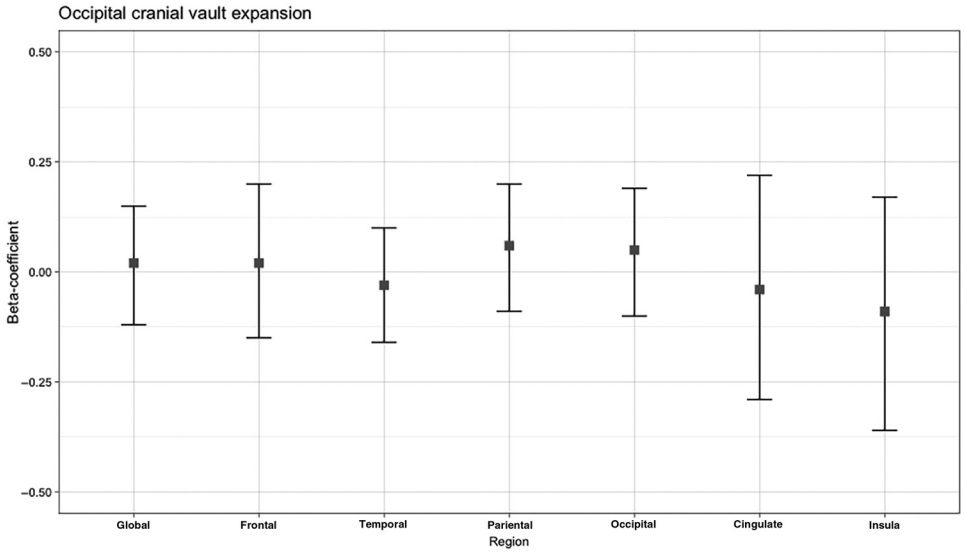


**Fig. 1.** β-coefficients with 95% confidence intervals associated with occipital cranial vault expansion extracted from linear mixed models of each lobe as well as globally.

difference in cortical thickness (0.37 mm), far exceeding that previously reported as a result of papilledema, between surgical treatment groups. With improved power we would expect more subtle cortical thickness changes to emerge, congruent with previous findings.

Our secondary analysis showed lambdoid synostosis to result in thinning across all brain regions, with pronounced effects in the cingulate and frontal cortices. We expected to observe greater effect sizes between synostoses and corresponding cortical lobes (eg, coronal/frontal, lambdoid/occipital), but interestingly lambdoid involvement was associated with more thinning in the frontal cortex than the occipital. The largest effect sizes observed were those of lambdoid synostoses on the cingulate gyri. To date, lambdoid synostoses have been shown to result in localized brain dysmorphology such as increased rates of cerebellar tonsillar herniation.[33,34] This is likely due to the disproportionate cerebellar growth, which normally occurs in the first 2 years of life, in the context of posterior fossa maldevelopment.[35] It may be that the association between lambdoid craniosynostosis and cortical thinning is related to increased ICH rates, which then differentially affects more susceptible cortical regions such as the cingulate gyri. The explanation for why ICH rates may be elevated in lambdoid synostosis is crowding of the posterior fossa leading to venous outflow obstruction and/or accessory venous drainage pathways, which are common in CP syndrome.[36] Furthermore, contralateral growth restriction of the occiput may result in a cranial distortion mirrored by that of the pericallosal artery supplying the cingulate cortex; however, further study is needed to evaluate this possibility.

Coronal suture involvement was also associated with cortical thinning across all brain regions measured; however, its effects were generally small (Cohen's $d < 0.5$) except for frontal lobes. But even in frontal lobes, the effect was not definitive, as 95% confidence intervals included zero at their outer limits. Despite this, it seems that some localized influence does exist and a more comprehensive explanation is required to resolve these apparent discrepancies. Due to the fact that lambdoid and coronal synostosis both result in significant skull distortion, including flattening of the occiput, scoliosis of the face and turribrachycephaly, dependent upon specific suture combinations, we must consider the influence of overall cranial shape and its contribution to ICH and subsequent cortical changes. It may be that turribrachycephaly contributes to frontal cortical thinning, which occurs in bicoronal and bilambdoid synostosis, while isolated lambdoid suture involvement contributes more heavily to ICH development, disproportionately impacting the cingulate gyri. The idea that cranial shape influences neurodevelopment is supported by previous study in non-syndromic craniosynostosis patients who experienced worse developmental and linguistic outcomes than healthy children or patients with varying forms of single suture synostosis.[37–40] Our results similarly show cortical thickness effect sizes corresponding to these outcomes, with sagittal synostosis resulting in increased cortical thickness across various brain regions, most notably in the occipital lobes.

When interpreting the results of our study, several limitations should be considered. First, 34 patients were included for analysis, which limits the power of our study to draw negative inferences and could explain our failure to discover any cortical changes associated with type of primary cranial vault expansion. Almost all scans were postoperative in this study. Ideally, cortical thickness data pre and postoperatively would be obtained from serial imaging studies; however, this was not possible due to the early age of surgery (median 1.27 years) and the lack of adequate tissue contrast inherent in infant brains on MRI.[41] Additionally, it is possible that other variables unaccounted for in our analysis, which may influence

**Table 3. Cohen's *d* Effect Sizes with SD and 95% Confidence Intervals for Suture Involvement on Cortical Thickness by Lobe and Hemisphere**

| | Left Coronal | Right Coronal | Sagittal | Left Lambdoid | Right Lambdoid |
|---|---|---|---|---|---|
| N | 26 | 28 | 23 | 23 | 25 |
| Male (%) | 14 (54%) | 15 (54%) | 14 (61%) | 13 (57%) | 14 (56%) |
| Female (%) | 12 (46%) | 13 (46%) | 9 (39%) | 10 (43%) | 11 (44%) |
| Median age (SD) | 8.0 (4.7) | 8.6 (4.7) | 10.7 (3.6) | 8.0 (4.6) | 8.0 (4.6) |
| Left frontal | | | | | |
| Cohen's *d* | −0.56 | −0.31 | 0.03 | −0.48 | −0.65 |
| Sd | 0.20 | 0.20 | 0.20 | 0.20 | 0.19 |
| Conf.int.lower | −1.40 | −1.22 | −0.71 | −1.24 | −1.46 |
| Conf.int.upper | 0.27 | 0.61 | 0.78 | 0.28 | 0.16 |
| Right frontal | | | | | |
| Cohen's *d* | −0.65 | −0.42 | 0.23 | −0.53 | −0.59 |
| Sd | 0.19 | 0.19 | 0.19 | 0.19 | 0.19 |
| Conf.int.lower | −1.49 | −1.34 | −0.52 | −1.28 | −1.40 |
| Conf.int.upper | 0.19 | 0.50 | 0.98 | 0.23 | 0.21 |
| Left temporal | | | | | |
| Cohen's *d* | −0.52 | −0.06 | 0.11 | −0.56 | −0.32 |
| Sd | 0.15 | 0.15 | 0.15 | 0.15 | 0.15 |
| Conf.int.lower | −1.36 | −0.98 | −0.64 | −1.32 | −1.12 |
| Conf.int.upper | 0.31 | 0.85 | 0.85 | 0.20 | 0.47 |
| Right temporal | | | | | |
| Cohen's *d* | −0.24 | −0.01 | −0.09 | −0.43 | −0.24 |
| Sd | 0.16 | 0.16 | 0.16 | 0.16 | 0.16 |
| Conf.int.lower | −1.07 | −0.92 | −0.83 | −1.18 | −1.04 |
| Conf.int.upper | 0.58 | 0.91 | 0.66 | 0.32 | 0.55 |
| Left parietal | | | | | |
| Cohen's *d* | −0.42 | −0.25 | −0.37 | −0.05 | −0.24 |
| Sd | 0.15 | 0.15 | 0.15 | 0.15 | 0.15 |
| Conf.int.lower | −1.25 | −1.17 | −1.13 | −0.80 | −1.03 |
| Conf.int.upper | 0.41 | 0.66 | 0.38 | 0.70 | 0.56 |
| Right parietal | | | | | |
| Cohen's *d* | −0.37 | −0.20 | −0.12 | −0.30 | −0.50 |
| Sd | 0.16 | 0.16 | 0.16 | 0.16 | 0.16 |
| Conf.int.lower | −1.20 | −1.11 | −0.87 | −1.05 | −1.30 |
| Conf.int.upper | 0.46 | 0.72 | 0.63 | 0.45 | 0.30 |
| Left occipital | | | | | |
| Cohen's *d* | −0.34 | −0.10 | 0.70 | −0.07 | −0.30 |
| Sd | 0.19 | 0.20 | 0.19 | 0.20 | 0.19 |
| Conf.int.lower | −1.17 | −1.02 | −0.07 | −0.82 | −1.10 |
| Conf.int.upper | 0.49 | 0.81 | 1.47 | 0.68 | 0.49 |
| Right occipital | | | | | |
| Cohen's *d* | −0.31 | −0.06 | 0.78 | −0.09 | −0.22 |
| Sd | 0.19 | 0.20 | 0.18 | 0.20 | 0.20 |
| Conf.int.lower | −1.13 | −0.97 | 0.01 | −0.84 | −1.01 |
| Conf.int.upper | 0.52 | 0.86 | 1.55 | 0.66 | 0.58 |
| Left cingulated | | | | | |
| Cohen's *d* | −0.43 | −0.36 | 0.16 | −0.87 | −1.23 |
| Sd | 0.27 | 0.27 | 0.27 | 0.25 | 0.24 |
| Conf.int.lower | −1.26 | −1.28 | −0.59 | −1.65 | −2.08 |
| Conf.int.upper | 0.40 | 0.56 | 0.90 | −0.10 | −0.38 |
| Right cingulated | | | | | |
| Cohen's *d* | −0.32 | −0.11 | 0.49 | −1.00 | −1.05 |
| Sd | 0.33 | 0.33 | 0.32 | 0.30 | 0.30 |
| Conf.int.lower | −1.14 | −1.03 | −0.27 | −1.78 | −1.88 |
| Conf.int.upper | 0.51 | 0.81 | 1.25 | −0.21 | −0.22 |
| Left insula | | | | | |
| Cohen's *d* | −0.57 | −0.27 | 0.21 | −0.30 | −0.31 |
| Sd | 0.33 | 0.34 | 0.34 | 0.34 | 0.34 |
| Conf.int.lower | −1.40 | −1.19 | −0.53 | −1.05 | −1.10 |
| Conf.int.upper | 0.27 | 0.64 | 0.96 | 0.45 | 0.49 |
| Right insula | | | | | |
| Cohen's *d* | −0.66 | −0.20 | 0.24 | −0.46 | −0.30 |
| Sd | 0.32 | 0.33 | 0.33 | 0.33 | 0.33 |
| Conf.int.lower | −1.50 | −1.12 | −0.51 | −1.22 | −1.09 |
| Conf.int.upper | 0.18 | 0.72 | 0.99 | 0.29 | 0.50 |

cortical development, could have resulted in reverse confounding, thereby masking any effect of surgical intervention type. Finally, the precision of FreeSurfer processing methodologies may be influenced by cranial dysmorphology. FreeSurfer generates maps using spatial intensity gradients across tissue classes on MRI data, which allow for greater resolution than voxel size. Previous validation of FreeSurfer has demonstrated cortical thickness measurement to be statistically indistinguishable from traditional neuropathology techniques on histological analysis.[26,27,30] Furthermore, FreeSurfer analysis has been applied with accuracy to a variety of neuropathologies, across a variety of ages.[27,29,42] In this study we confirmed successful processing through manual inspection of all surfaces generated by the FreeSurfer pipeline on each scan to ensure the reliability of our data.

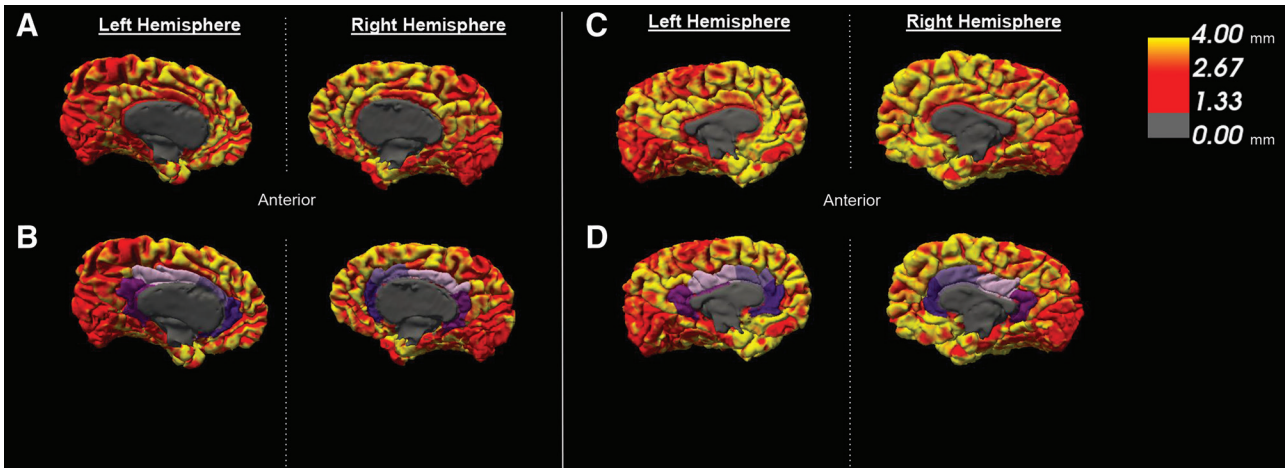


**Fig. 2.** Pial surface heat maps extracted from FreeSurfer with 0–4 mm cortical thickness scale. A, Left and right hemispheres of a 9-year-old CP patient with bilateral lambdoid synostosis. B, Hemispheres of the same patient in A, with cingulate gyri identified in purple. C, Left and right hemispheres of a 7-year-old CP patient with bicoronal synostosis. D, Hemispheres of the same patient in C, with cingulate gyri identified in purple.

Despite variable effects of synostosis pattern on regional cortical thickness seen in this study, we observed similar global and regional thicknesses in both frontal-first and occipital-first cranial vault expansion groups. Evaluation of effect size due to suture involvement showed frontal lobe thinning in coronal and lambdoid synostosis cases, suggesting that turribrachycephaly may adversely influence frontal cortex development. Lambdoid synostosis was also associated with a pronounced thinning effect in the cingulate gyri, likely attributable to increased ICH rates due to crowding of the posterior fossa. This explanation seems most likely, given the buried nature of the cingulate cortex as well as its associations with the cerebellum, and frequent tonsillar herniation seen in lambdoid CP cases.[43,44] Future studies should evaluate the effect of primary cranial vault expansion type as well as synostosis pattern on neuropsychological and functional outcomes such as hearing as well as investigate potential vascular causes of cingulate thinning observed in this study.

***Alexander T. Wilson***
Department of Plastic and Reconstructive Surgery
Erasmus Medical Center
Doctor Molewaterplein 40
3015 GD Rotterdam, the Netherlands
E-mail: a.wilson@erasmusmc.nl

## ACKNOWLEDGMENT

*This publication was made possible by the Richard K. Gershon Student Research Fellowship at Yale University School of Medicine.*

## REFERENCES

1. Cohen MM Jr, Kreiborg S. Birth prevalence studies of the Crouzon syndrome: comparison of direct and indirect methods. *Clin Genet*. 1992;41:12–15.
2. Rutland P, Pulleyn LJ, Reardon W, et al. Identical mutations in the FGFR2 gene cause both Pfeiffer and Crouzon syndrome phenotypes. *Nat Genet*. 1995;9:173–176.
3. Ghali GZ, Zaki Ghali MG, Ghali EZ, et al. Intracranial venous hypertension in craniosynostosis: mechanistic underpinnings and therapeutic implications. *World Neurosurg*. 2019;127:549–558.
4. Spruijt B, Mathijssen IM, Bredero-Boelhouwer HH, et al. Sleep architecture linked to airway obstruction and intracranial hypertension in children with syndromic craniosynostosis. *Plast Reconstr Surg*. 2016;138:1019e–1029e.
5. Cinalli G, Sainte-Rose C, Kollar EM, et al. Hydrocephalus and craniosynostosis. *J Neurosurg*. 1998;88:209–214.
6. Spruijt B, Joosten KF, Driessen C, et al. Algorithm for the management of intracranial hypertension in children with syndromic craniosynostosis. *Plast Reconstr Surg*. 2015;136:331–340.
7. Spruijt B, Rijken BF, den Ottelander BK, et al. First vault expansion in apert and Crouzon-Pfeiffer syndromes: front or back? *Plast Reconstr Surg*. 2016;137:112e–121e.
8. Burgaleta M, Johnson W, Waber DP, et al. Cognitive ability changes and dynamics of cortical thickness development in healthy children and adolescents. *Neuroimage*. 2014;84:810–819.
9. Karama S, Ad-Dab'bagh Y, Haier R, et al. Positive association between cognitive ability and cortical thickness in a representative US sample of healthy 6 to 18 year-olds. *Intelligence*. 2009;37:145–155.
10. Duncan NW, Gravel P, Wiebking C, et al. Grey matter density and GABAA binding potential show a positive linear relationship across cortical regions. *Neuroscience*. 2013;235:226–231.
11. Williams VJ, Juranek J, Cirino P, et al. Cortical thickness and local gyrification in children with developmental dyslexia. *Cereb Cortex*. 2018;28:963–973.
12. Gautam P, Anstey KJ, Wen W, et al. Cortical gyrification and its relationships with cortical volume, cortical thickness, and cognitive performance in healthy mid-life adults. *Behav Brain Res*. 2015;287:331–339.
13. Alvarez I, Parker AJ, Bridge H. Normative cerebral cortical thickness for human visual areas. *Neuroimage*. 2019;201:116057.
14. Zink DN, Miller JB, Caldwell JZK, et al. The relationship between neuropsychological tests of visuospatial function and lobar cortical thickness. *J Clin Exp Neuropsychol*. 2018;40:518–527.
15. Menary K, Collins PF, Porter JN, et al. Associations between cortical thickness and general intelligence in children, adolescents and young adults. *Intelligence*. 2013;41:597–606.

16. Wilson AT, Den Ottelander BK, De Goederen R, et al. Intracranial hypertension and cortical thickness in syndromic craniosynostosis. *Dev Med Child Neurol.* 2020;62:799–805.
17. Abu-Sittah GS, Jeelani O, Dunaway D, et al. Raised intracranial pressure in Crouzon syndrome: incidence, causes, and management. *J Neurosurg Pediatr.* 2016;17:469–475.
18. Fernandes MB, Maximino LP, Perosa GB, et al. Apert and Crouzon syndromes-Cognitive development, brain abnormalities, and molecular aspects. *Am J Med Genet A.* 2016;170:1532–1537.
19. Maliepaard M, Mathijssen IM, Oosterlaan J, et al. Intellectual, behavioral, and emotional functioning in children with syndromic craniosynostosis. *Pediatrics.* 2014;133:e1608–e1615.
20. Rijken BF, Leemans A, Lucas Y, et al. Diffusion tensor imaging and fiber tractography in children with craniosynostosis syndromes. *AJNR Am J Neuroradiol.* 2015;36:1558–1564.
21. Mathijssen IM. Guideline for care of patients with the diagnoses of craniosynostosis: working group on craniosynostosis. *J Craniofac Surg.* 2015;26:1735–1807.
22. Rijken BF, Lequin MH, van der Lijn F, et al. The role of the posterior fossa in developing Chiari I malformation in children with craniosynostosis syndromes. *J Craniomaxillofac Surg.* 2015;43:813–819.
23. Clarkson MJ, Cardoso MJ, Ridgway GR, et al. A comparison of voxel and surface based cortical thickness estimation methods. *Neuroimage.* 2011;57:856–865.
24. Fischl B, Sereno MI, Dale AM. Cortical surface-based analysis. II: inflation, flattening, and a surface-based coordinate system. *Neuroimage.* 1999;9:195–207.
25. Dale AM, Fischl B, Sereno MI. Cortical surface-based analysis. I. Segmentation and surface reconstruction. *Neuroimage.* 1999;9:179–194.
26. Fischl B, Dale AM. Measuring the thickness of the human cerebral cortex from magnetic resonance images. *Proc Natl Acad Sci U S A.* 2000;97:11050–11055.
27. Rosas HD, Liu AK, Hersch S, et al. Regional and progressive thinning of the cortical ribbon in Huntington's disease. *Neurology.* 2002;58:695–701.
28. Kuperberg GR, Broome MR, McGuire PK, et al. Regionally localized thinning of the cerebral cortex in schizophrenia. *Arch Gen Psychiatry.* 2003;60:878–888.
29. Salat DH, Buckner RL, Snyder AZ, et al. Thinning of the cerebral cortex in aging. *Cereb Cortex.* 2004;14:721–730.
30. Cardinale F, Chinnici G, Bramerio M, et al. Validation of FreeSurfer-estimated brain cortical thickness: comparison with histologic measurements. *Neuroinformatics.* 2014;12:535–542.
31. Martinussen M, Fischl B, Larsson HB, et al. Cerebral cortex thickness in 15-year-old adolescents with low birth weight measured by an automated MRI-based method. *Brain.* 2005;128(pt 11):2588–2596.
32. Bjuland KJ, Løhaugen GC, Martinussen M, et al. Cortical thickness and cognition in very-low-birth-weight late teenagers. *Early Hum Dev.* 2013;89:371–380.
33. Chivoret N, Arnaud E, Giraudat K, et al. Bilambdoid and sagittal synostosis: report of 39 cases. *Surg Neurol Int.* 2018;9:206.
34. Fearon JA, Dimas V, Ditthakasem K. Lambdoid craniosynostosis: the relationship with chiari deformations and an analysis of surgical outcomes. *Plast Reconstr Surg.* 2016;137:946–951.
35. Cinalli G, Renier D, Sebag G, et al. Chronic tonsillar herniation in Crouzon's and Apert's syndromes: the role of premature synostosis of the lambdoid suture. *J Neurosurg.* 1995;83:575–582.
36. Hayward R. Venous hypertension and craniosynostosis. *Childs Nerv Syst.* 2005;21:880–888.
37. Korpilahti P, Saarinen P, Hukki J. Deficient language acquisition in children with single suture craniosynostosis and deformational posterior plagiocephaly. *Childs Nerv Syst.* 2012;28:419–425.
38. Andrews BT, Fontana SC. Correlative vs. causative relationship between neonatal cranial head shape anomalies and early developmental delays. *Front Neurosci.* 2017;11:708.
39. Renier D, Lajeunie E, Arnaud E, et al. Management of craniosynostoses. *Childs Nerv Syst.* 2000;16:645–658.
40. Da Costa AC, Anderson VA, Savarirayan R, et al. Neurodevelopmental functioning of infants with untreated single-suture craniosynostosis during early infancy. *Childs Nerv Syst.* 2012;28:869–877.
41. Wang F, Lian C, Wu Z, et al. Developmental topography of cortical thickness during infancy. *Proc Natl Acad Sci U S A.* 2019;116:15855–15860.
42. Nickel K, Tebartz van Elst L, Manko J, et al. Inferior frontal gyrus volume loss distinguishes between autism and (comorbid) attention-deficit/hyperactivity disorder-a freesurfer analysis in children. *Front Psychiatry.* 2018;9:521.
43. Badura A, Verpeut JL, Metzger JW, et al. Normal cognitive and social development require posterior cerebellar activity. *Elife* 2018;7:e36401.
44. Herrojo Ruiz M, Maess B, Altenmüller E, et al. Cingulate and cerebellar beta oscillations are engaged in the acquisition of auditory-motor sequences. *Hum Brain Mapp.* 2017;38:5161–5179.